Modal Analysis of Turborotors Using Planar Modes—Theory

by E. J. GUNTER, K. C. CHOY
Department of Mechanical Engineering
University of Virginia, Charlottesville, Virginia 22901, *U.S.A.*

ABSTRACT: *The generalized dynamic equations of motion have been obtained by the direct stiffness method for multimass flexible rotor bearing systems including the effects of gyroscopic moments, disc skew, and rotor acceleration. A set of undamped critical speed mode shapes calculated from the average horizontal and vertical bearing stiffness is used to transform the equations of motion into a set of coupled modal equations of motion. The modal equations are coupled by the generalized bearing coefficients and the gyroscopic moments. An analysis using only undamped critical speeds or decoupled modal analysis assuming proportional damping may lead to erroneous results. This paper presents a rapid method of calculating rotor resonance speeds with their corresponding amplification factors, stability and unbalance response of turborotors. Examples of the application of this modal approach are presented and results are compared to those of other methods such as matrix transfer analysis.*

Notation

A_c	Rotor amplification factor of the ith undamped critical speed
A_i	Modal constant coefficients
A_{ui}	Rotor amplification factor at ith resonance speed
$[B^x]$, $[B^y]$	Additional modal support stiffness matrix
$[C^x]$, $[C^y]$	Modal support damping matrix
$[C_B]$	Complete support damping Matrix
$[C_G]$	Gyroscopic damping matrix
$[D^x]$, $[D^y]$	Cross-coupled modal support and gyroscopic damping matrix
$[E^x]$, $[E^y]$	Cross-coupled modal support and disc acceleration stiffness matrix
E_i	Young's modulus of the ith shaft element
$\{F(t)\}$	External time dependent force and moment forcing function vector
$\{F_x(t)\}$, $\{F_y(t)\}$	External time dependent force vector
F_{bx}, F_{by}	Generalized bearing forces
I_i	Moment of inertia of ith shaft element
$[I]$	Identity matrix
$[I_T]$	Diagonal transverse moment of inertia matrix
$[I_p]$	Diagonal polar moment of inertia matrix
$[K_A]$	Acceleration stiffness matrix

$[K_B]$	Complete bearing stiffness matrix
$[K_b]$	Average vertical and horizontal principal bearing stiffness matrix
$[K_s]$	Shaft stiffness matrix
L_i	Length of the ith shaft element
m_i	Concentrated mass at ith station
$[\bar{M}]$	Complete mass and inertia matrix
$[M]$	Concentrated mass matrix
$\{M_x(t)\}$, $\{M_y(t)\}$	External time dependent moment vector
M_{bx}, M_{by}	Generalized bearing moment
P_i	Real part of the ith damped complex eigenvalue
$\{P_x\}$, $\{P_y\}$	Modal unbalance forcing function vector
$\{q_x\}$, $\{q_y\}$	Time dependent modal coefficient vector
$\{U\}$	Total displacement vector
$\{X\}$, $\{Y\}$	Translational displacement vector
α_i	Phase angle of rotor unbalance to reference at ith station
β_i	Phase angle of maximum disc skew to reference mark at ith station
λ_i	Damped complex frequency $= p_i + i\omega_{di}$ (rad/sec) of the ith mode
$\{\Phi_i\} = \begin{pmatrix}(\phi_i)\\(\phi_i')\end{pmatrix}$	Orthonormal mode of the ith undamped critical speed
$[\Phi] = [\{\phi_1\}, \{\phi_2\}\ldots]$	Complete orthonormal mode matrix
ω_{di}	Damped natural frequency, (rad/sec) of the ith mode
ω_{ci}	Rotor undamped critical speed of the ith mode
ω_p	Critical speed of planar mode
ω_{ui}	Rotor peak unbalance response speed, (rad/sec) of the ith mode
ω	Rotor operating speed, (rad/sec)
$[\Lambda] = [\omega_i^2]$	Diagonal undamped critical speed matrix
ξ_i	Modal damping ratio of the ith mode

I. Introduction

In the design of modern gas turbines and other high speed turbomachinery, it is often necessary for the machinery to operate through several rotor critical speeds in order to reach its full power operating level. Complete rotor analysis includes damped critical speeds, stability analysis, unbalance response, and transient motion of the rotor system. A number of recent works (**1–24**) have developed various methods of obtaining the different types of rotor motion.

The homogeneous solution of the damped equations of motion is a complex eigenvalue problem, and the damped system complex frequencies may be determined numerically by various finite element or matrix transfer procedures as outlined by Ruhl (**7**), and Lund (**11**). The determination of the damped system complex frequencies is a considerably more difficult problem than the determination of the undamped modes by the Prohl–Myklestad matrix transfer method (**24**). For rotor systems with a large number of mass station, the complex eigenvalue procedure may run into numerical difficulties (**16**).

Another important design characteristic of a rotor is the sensitivity of the

system to unbalance. The peak unbalance responses are assumed to occur at the rotor critical speeds. It is not readily apparent from the examination of the undamped rotor modes what the magnitude of each critical speed amplification factor might be. The determination of the rotor synchronous unbalance response may be evaluated by various matrix transfer methods such as developed by Lund (**4**) and others (**3, 6**). However, to fully evaluate the rotor unbalance response through several critical speeds, it is necessary to calculate the rotor response with various distributions of rotor unbalance to insure excitation of the various critical speed modes. The calculation of the rotor response with various unbalance distributions may be quite time consuming. These calculations do not furnish the designers with readily attainable fundamental design parameters to optimize the rotor supports for minimum amplitude and bearing force over the desired operating speed range.

The general damped equations of motion for a multimass rotor are often difficult and expensive to solve by direct methods. One approach, which has been proven successful at avoiding some of the problems is the modal method (**2, 3, 5, 8, 9, 12, 13, 17–24**). The modal method reduces the number of degrees of freedom of the system. In addition, much information about the rotor can be obtained by the calculation of modal properties, particularly if the modes can be decoupled in some manner.

In some cases, such as electric generators, the equations of motion can be decoupled easily (**5, 9, 20**) into horizontal and vertical modes making the analysis much easier than solving the general problem. Normally these systems are characterized by bearings being located near node points so that damping effects are small and can be considered proportional in nature. Other coupling forces can also be neglected. The resulting relatively simple mode shapes contribute to such developments as modal balancing. Unfortunately, most rotors do not fall into this class (**18, 19**).

Modal analyses have been carried out using free–free mode shapes (**12, 13, 18**). This has the advantage of developing mode shapes which are based solely on rotor geometric properties. Other factors such as bearing dynamic coefficients, which are functions of rotor speed, can be omitted until the overall rotor analysis. The same free–free mode shapes can be used for system critical speed, stability, unbalance response, and transient analysis. For most industrial rotors, this has the disadvantage that bearings, seals, and other forces can strongly affect rotor motion. So the free–free modes may not represent the rotor motion well. This leads to large numbers of modes being required for the analysis and difficulties with understanding rotor vibration problems.

This work develops a modal analysis for rotor systems using uncoupled undamped mode shapes including average bearing (or seal) linearized stiffness properties. These mode shapes are relatively easy to obtain (computer codes to accomplish this are widely available in industry) and are planar in form. Much more physical "feel" for the rotor motion is possible than with free–free modes, but the coupling terms must not be neglected in the full system analysis. A complete set of equations of motion are developed for the shaft including gyroscopics, skewed discs, and full bearing dynamic coefficients. The planar

modes are then used to obtain damped natural frequencies and forced response. The use of the complete method is demonstrated by its application to an industrial 8 stage compressor.

II. Modal Theory

1. *Planar Undamped Modes*

It is desired to obtain a single set of planar undamped modes incorporating an average bearing stiffness for modal analysis. The shaft is assumed symmetric, rotor gyroscopic effects are neglected, bearing damping is neglected, and only an average bearing principal stiffness term is considered. As shown in the Appendix, the equations for the planar undamped mode shapes are

$$\begin{bmatrix}[M] & 0\\ 0 & [I_t]\end{bmatrix}\begin{Bmatrix}\ddot{X}\\ \ddot{\theta}\end{Bmatrix}+\begin{bmatrix}[K_b] & 0\\ 0 & 0\end{bmatrix}\begin{Bmatrix}X\\ \theta\end{Bmatrix}+\begin{bmatrix}[k_{xx}] & [k_{x\theta}]\\ [k_{\theta x}] & [k_{\theta\theta}]\end{bmatrix}\begin{Bmatrix}X\\ \theta\end{Bmatrix}=\begin{Bmatrix}0\\ 0\end{Bmatrix} \tag{2.1}$$

where

$$[K_b]=\frac{[K_{xx}]_B+[K_{yy}]_B}{2}.$$

The average bearing stiffness is taken from K_{bxx} and K_{byy} evaluated for a single speed in the operating speed range.

The generalized displacement vector $\{U\}$ is represented by the expansion of the undamped modes obtained from a solution of Eq. (A.11) as

$$\{U\}=\sum_{i=1}^{n}\begin{Bmatrix}(q_{xi}\Phi_i)\\ (q_{yi}\Phi_i)\end{Bmatrix}. \tag{2.2}$$

From Eq. (A. 13) in the Appendix, the equations of motion can be written, using modal co-ordinates, as

$$\begin{Bmatrix}(\ddot{q}_x)\\ (\ddot{q}_y)\end{Bmatrix}+\begin{bmatrix}[C^x] & [D^x]\\ [D^y] & [C^y]\end{bmatrix}\begin{Bmatrix}(\dot{q}_x)\\ (\dot{q}_y)\end{Bmatrix}+\begin{bmatrix}[B^x] & [E^x]\\ [E^y] & [B^y]\end{bmatrix}\begin{Bmatrix}(q_x)\\ (q_y)\end{Bmatrix}+\begin{bmatrix}[\Lambda] & [0]\\ [0] & [\Lambda]\end{bmatrix}\begin{Bmatrix}(q_x)\\ (q_y)\end{Bmatrix}=\begin{Bmatrix}(0)\\ (0)\end{Bmatrix}. \tag{2.3}$$

It should be clear that this general modal formulation is not restricted to the particular set of mode shapes obtained by solving Eq. (2.1).

2. *Uncoupled Damped Modal Analysis*

In order to uncouple the modal equations, it is often the practice that gyroscopic effects and the support cross-coupled stiffness and damping values in the general damping matrix are assumed to be small or using the standard assumption in structural mechanics that the damping matrix is proportional to the mass or stiffness matrix by some linear relationship (**21**). The expression is

$$[C^x]=a\begin{bmatrix}[M] & [0]\\ [0] & [I_t]\end{bmatrix}+b\begin{bmatrix}[k_{xx}+K_b] & [k_{x\theta}]\\ [k_{\theta x}] & [k_{\theta\theta}]\end{bmatrix} \tag{2.4}$$

where a and b are arbitrary constants. This assumption uncouples the modal equations of motion which are relatively easy to analyze but often not accurate for turbomachinery with fluid film bearings or seals.

Using the above assumption, the modal equation can be reduced to its standard form (**5, 9, 20**) as

$$\ddot{q}_{xi} + 2\xi_i\omega_i\dot{q}_{xi} + \omega_i^2 q_{xi} = F_{xi}\,. \tag{2.5}$$

Assuming a solution of the form

$$q_{xi} = \bar{A}_i e^{\lambda t}$$

the homogeneous solution yields the complex eigenvalues

$$\lambda_{1,2} = P_i \pm i\omega_{di} = -\xi_i\omega_i \pm i\omega_i\sqrt{(1-\xi_i^2)} \tag{2.6}$$

where ω_{di} is the damped critical speed.

If F_{xi} is sinusoidal forcing function due to unbalance, a symchronous response solution is easily found. It can be shown that the peak rotor unbalance response does not occur at the undamped critical speed ω_i or at the damped critical speed ω_{di} but at a speed ω_{ui} given by (**10**) similar to that for a single mass rotor.

$$\omega_{ui} = \frac{\omega_i}{\sqrt{(1-2\xi_i^2)}} \tag{2.7}$$

or if the complex eigenvalues for the damped system are known

$$\omega_{ui} = \frac{\omega_{di}^2 + p_i^2}{\sqrt{\omega_{di}^2 - p_i^2)}}\,. \tag{2.8}$$

The rotor amplification factor for the peak rotor unbalance response is given by (**10**)

$$A_{ui} = \frac{1}{2\xi_i\sqrt{(1-\xi_i^2)}} \tag{2.9}$$

or

$$A_{ui} = \frac{\omega_{di}^2 + p_i^2}{-2P_i\omega_{di}}\,. \tag{2.10}$$

Therefore it is seen for the case of the uncoupled modal analysis that if the modal damping or complex eigenvalues can be calculated and the damping is proportional, then the speed at which the maximum unbalance response occurs can be predicted along with the rotor amplification factor.

Although the above equations for the prediction of the rotor peak unbalance response speeds and amplification factors provide insight into rotor behavior, for realistic turborotors with fluid film bearings and gyroscopic moment coupling, the modal equations of motion cannot be simply uncoupled, as Bishop and Parkinson have done (**9, 20**), but the modal equations must be simultaneously considered for both the x-z and y-z planes of motion as Childs has demonstrated (**12, 13**). The general coupled modal analysis to determine the stability

of the damped natural frequencies (eigenvalues) is discussed in the following section.

3. *Coupled Damped Modal Analysis*

It is apparent that the damped critical speeds predict considerably different behavior of the rotor system than does the analysis using undamped critical speeds. There are however, several problems involved with the calculation of the complex eigenvalues. At present, there are few damped critical speed computer programs generally available for usage and second, considerable numerical difficulties have been found in various programs in the simulation of large multistation machines. There is, however, a procedure in which the damped critical speeds may be rapidly and accurately calculated by using the undamped modes. This can be achieved by solving the modal equations of motion in (2.3) by looking for a solution of the form

$$\begin{Bmatrix}(q_x)\\(q_y)\end{Bmatrix}=\begin{Bmatrix}(\bar{A}_x)\\(\bar{A}_y)\end{Bmatrix}e^{\lambda t}$$

where λ is the complex damped natural frequency. Thus, Eq. (2.3) can be written as

$$\begin{bmatrix}\lambda^2[I]+\lambda[C^x]+[B^x]+[\Lambda] & \lambda[D^x]+[E^x]\\ \lambda[D^y]+[E^y] & \lambda^2[I]+\lambda[C^y]+[B^y]+[\Lambda]\end{bmatrix}\begin{Bmatrix}(\bar{A}_x)\\(\bar{A}_y)\end{Bmatrix}=0\,. \tag{2.11}$$

The above matrix equation can be expanded into standard eigenvalue form as

$$\begin{bmatrix}\lambda[I] & 0 & 0 & 0\\ 0 & \lambda[I] & 0 & 0\\ 0 & 0 & \lambda[I] & 0\\ 0 & 0 & 0 & \lambda[I]\end{bmatrix}\begin{Bmatrix}\lambda(\bar{A}_x)\\ \lambda(\bar{A}_y)\\ (\bar{A}_x)\\ (\bar{A}_y)\end{Bmatrix}$$

$$-\begin{bmatrix}-[C^x] & -[D^x] & -[B^x+\Lambda] & -[E^x]\\ -[D^y] & -[C^y] & -[E^y] & -[B^y+\Lambda]\\ -[I] & 0 & 0 & 0\\ 0 & -[I] & 0 & 0\end{bmatrix}\begin{Bmatrix}\lambda(\bar{A}_x)\\ \lambda(\bar{A}_y)\\ (\bar{A}_x)\\ (\bar{A}_y)\end{Bmatrix}$$

$$=\begin{Bmatrix}(0)\\(0)\\(0)\\(0)\end{Bmatrix} \tag{2.12}$$

or in compact form as

$$\det[\lambda[I]-[A]]=0$$

which can be solved by eigenvalue procedure for complex eigenvalues or be expanded by Leverrier's Algorithm into a homogeneous polynomial equation

as

$$\lambda^{4n} + p_1\lambda^{4n-1} + p_2\lambda^{4n-2} + \ldots + p_{4n-1}\lambda + p_{4n} = 0 \tag{2.13}$$

where

$$p_1 = -\text{trace}\,[A]$$

$$p_k = -\frac{1}{k}\,\text{trace}\,[A\,B_{k-1}],\quad k = 2,\ 3,\ 4\ldots.,4n$$

$$[B_1] = [A] + p_1[I]$$

$$[B_k] = [A][B_{k-1}] + p_k[I],\quad k = 2,\ 3,\ 4\ldots.,4n\,.$$

With the above expanded polynomial, the stability of the system can be evaluated by either solving for the complex eigenvalue λ_i or by using the Routh stability criteria (**22**) (without actually solving for λ_i).

4 *Rotor Unbalance Response—Modal Method*

A rapid approach in computing the rotor forced response is by the modal method of analysis. This analysis is based on solving the modal forced equation of motion of (A.13) and (A.14) as derived in the Appendix. They are, in matrix form

$$\begin{Bmatrix}(\ddot{q}_x)\\(\ddot{q}_y)\end{Bmatrix} + \begin{bmatrix}[C^x] & [D^x]\\[D^y] & [C^y]\end{bmatrix}\begin{Bmatrix}(\dot{q}_x)\\(\dot{q}_y)\end{Bmatrix} + \begin{bmatrix}[B^x] & [E^x]\\[E^y] & [B^y]\end{bmatrix}\begin{Bmatrix}(q_x)\\(q_y)\end{Bmatrix} + \begin{bmatrix}[\Lambda] & [0]\\[0] & [\Lambda]\end{bmatrix}\begin{Bmatrix}(q_x)\\(q_y)\end{Bmatrix} = \begin{Bmatrix}(F_x)\\(F_y)\end{Bmatrix}. \tag{2.14}$$

While the time transient response of the rotor system can be solved by time integration of the modal equations, the steady state unbalance response can be solved by assuming a solution of the form

$$\begin{Bmatrix}(q_x)\\(q_y)\end{Bmatrix} = \begin{Bmatrix}(A_x)\\(A_y)\end{Bmatrix}e^{i\omega t}. \tag{2.15}$$

Without rotor acceleration, the forcing function in the x-direction for the ith mode can be expressed as

$$F_{xi} = \{\Phi_i\}^T\begin{Bmatrix}[m_i e_i]\\[\tau(I_p - I_t)]\end{Bmatrix}\omega^2 e^{i\omega t} = p_{xi}e^{i\omega t}. \tag{2.16}$$

Substituting the above relations into Eq. (2.14) results

$$\begin{bmatrix}-\omega^2[I] + i\omega(C^x] + [B^x] + [\Lambda] & i\omega[D^x] + [E^x]\\ i\omega[D^y] + [E^y] & -\omega^2[I] + i\omega[C^y] + B^y] + [\Lambda]\end{bmatrix}\begin{Bmatrix}(A_x)\\(A_y)\end{Bmatrix} = \begin{Bmatrix}(p_x)\\(p_y)\end{Bmatrix}. \tag{2.17}$$

The $\{A_x\}$ and $\{A_y\}$ can be solved simultaneously and the rotor motion can be

obtained by back substitution of these values into Eqs. (2.15) and (2.2) as

$$\{U\} = \begin{Bmatrix} (x) \\ (\theta) \\ (y) \\ (\psi) \end{Bmatrix} = \begin{bmatrix} [\Phi] & [0] \\ [0] & [\Phi] \end{bmatrix}$$

$$\begin{bmatrix} -\omega^2[I] + i\omega[C^x] + [B^x] + [\Lambda] & i\omega[D^x] + [E^x] \\ i\omega[D^y] + [E^y] & -\omega^2[I] + i\omega[C^y] + [B^y] + [\Lambda] \end{bmatrix}^{-1} \begin{Bmatrix} (p_x) \\ (p_y) \end{Bmatrix}. \quad (2.18)$$

It should be noted that the damped critical speed mode shapes may also be used to evaluate the rotor forced unbalance response by reducing the N second order equations of motion to $2N$ first-order equations as presented by Foss (**2**).

Modal transient response of the system can also be evaluated by numerical integration of the modal accelerations from Eq. (2.14) as

$$\begin{Bmatrix} (\ddot{q}_x) \\ (\ddot{q}_y) \end{Bmatrix} = \begin{Bmatrix} (F_x) \\ (F_y) \end{Bmatrix} - \begin{bmatrix} [C^x] & [D^x] \\ [D^y] & [C^y] \end{bmatrix} \begin{Bmatrix} (\dot{q}_x) \\ (\dot{q}_y) \end{Bmatrix} - \begin{bmatrix} [B^x + \Lambda] & [E^x] \\ [E^y] & [B^y + \Lambda] \end{bmatrix} \begin{Bmatrix} (q_x) \\ (q_y) \end{Bmatrix}. \quad (2.19)$$

The transient displacements of the system can be obtained by the transformation of the modal displacements as shown in Eq. (2.2).

III. Application on Industrial Compressor

To illustrate the application of the method, modal calculations are performed for an 8 stage centrifugal compressor as discussed by Lund (**11**) where damped natural frequency calculations were performed. The rotor weighs about 1400 lb and is 102 in. in length. The center of gravity of the rotor is almost midway between the two identical journal bearings of 5 in. diameter, 1.5 in. length and 0.0035 in. clearance. The bearing stiffness and damping coefficients used in this example (provided by Lund) are given in Table I. An undamped critical speed analysis with the average bearing stiffness of 609,550 lb/in. at the left bearing

TABLE I

Stiffness and damping coefficients.	Bearing number 1	2
K_{xx} (lb/in.)	441,000	415,300
K_{xy} (lb/in.)	83,330	88,540
K_{yx} (lb/in.	−853,500	−792,400
K_{yy} (lb/in.)	778,100	700,900
C_{xx} (lb/in.)	786.3	758.7
C_{xy} (lb–sec/in.)	−716.4	−674.3
C_{yx} (lb–sec/in.)	−716.4	−674.3
C_{yy} (lb/in.)	2,196.0	2,196.0

and 558,100 lb/in. at the right bearing indicates that the critical speeds will occur at 3270 RPM, 7527 RPM, 9018 RPM, 14,092 RPM, and 27,921 RPM. Note that the effects of bearing cross-coupled stiffness and rotor polar moments of inertia are neglected. The undamped mode shapes for this compressor are typical flexible rotor modes due to high stiffness of the bearings and the normalized mode shapes for the first five critical speeds are given in Figs. 1 and 2.

In order to illustrate the use of the modal equation derived in the previous

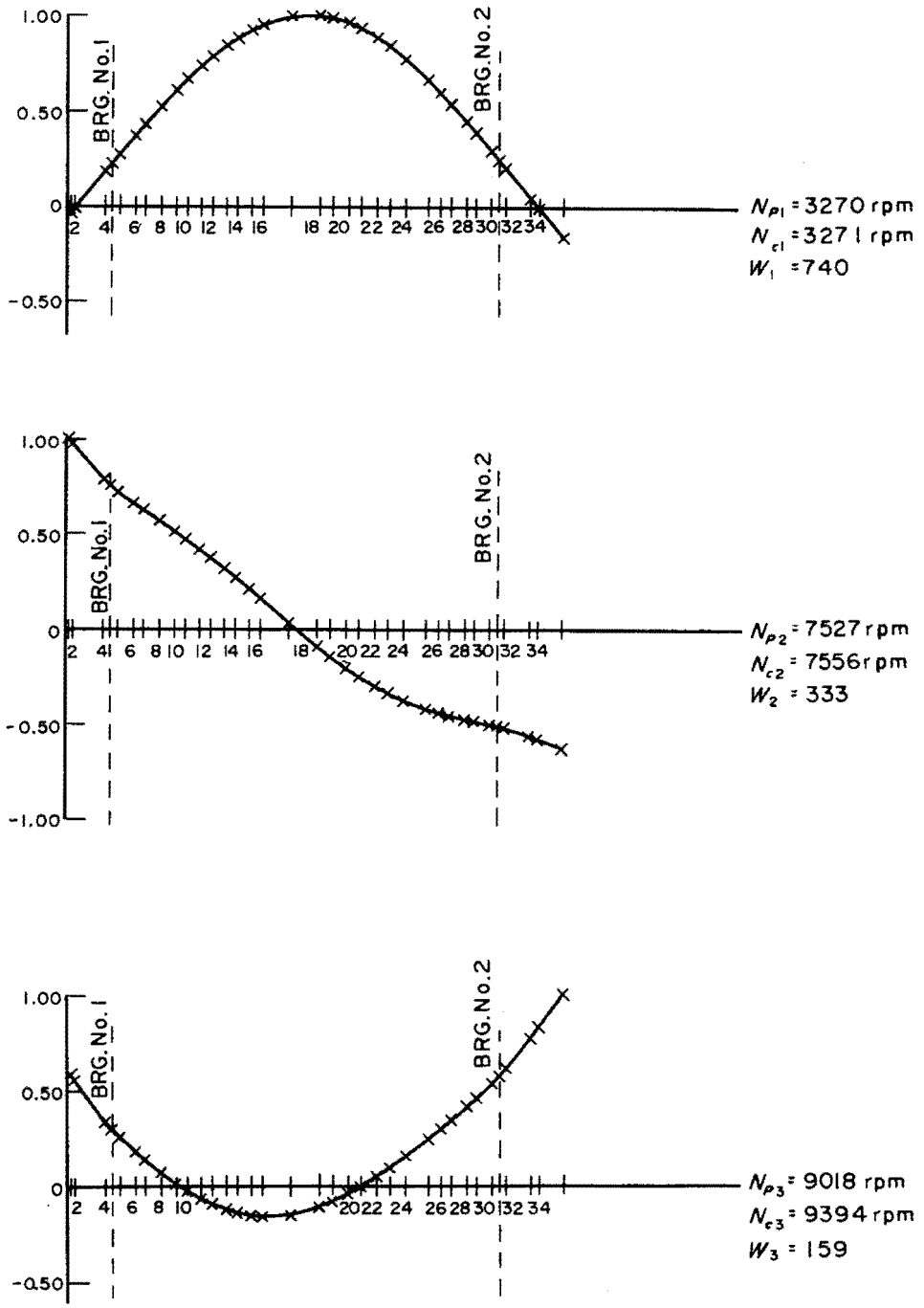

FIG. 1. First three undamped compressor planar mode shapes.

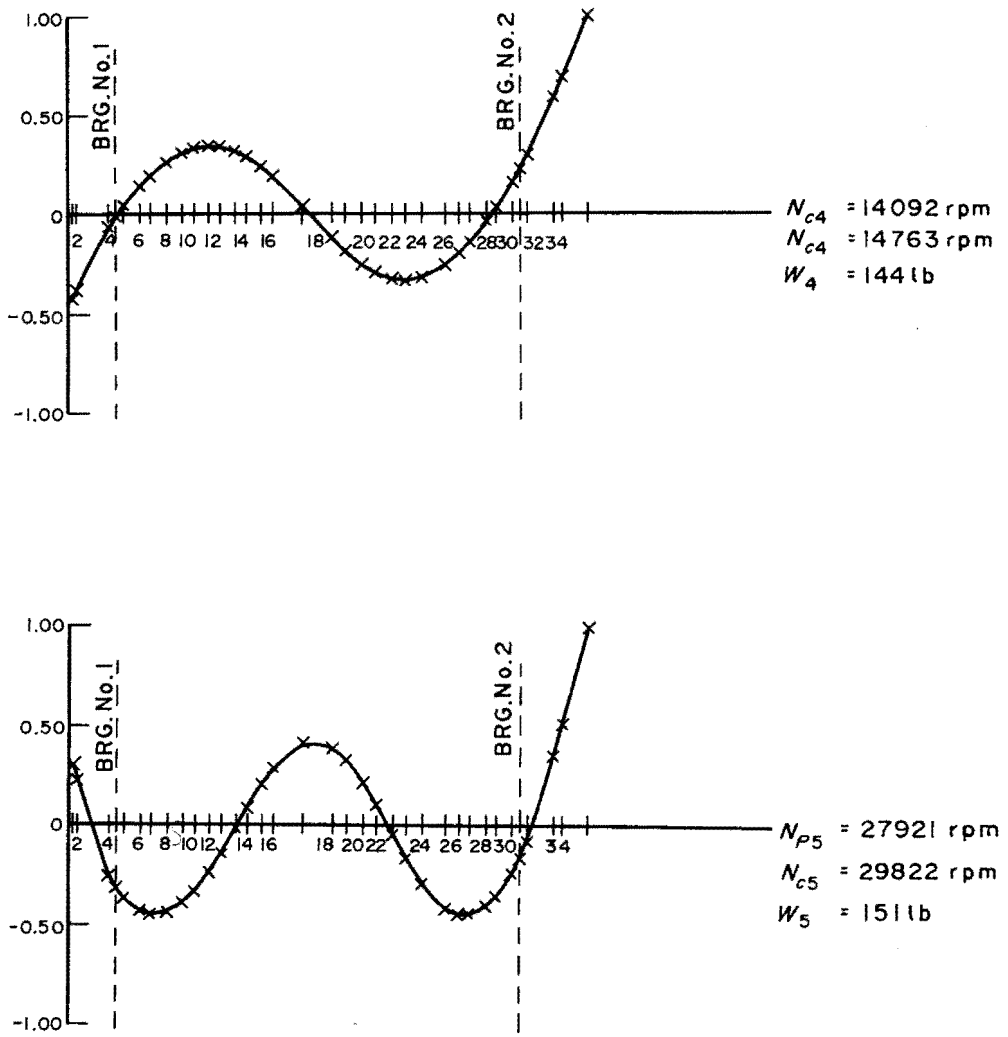

FIG. 2. 4th and 5th undamped compressor planar mode shapes.

section, the damped natural frequencies of the system were calculated with bearing cross-coupling stiffness and damping effects. A computer program was set up to formulate the standard eigenvalue matrix as given in Eq. (2.12) and the $4N$ degree polynomial equation of (2.13) was solved by Leverrier's Algorithm. Rotor speed of 3000 RPM is assumed for first critical speed calculation of disc gyroscopic effects and 6000 RPM for the second critical speed. Using the modal approach discussed in Section II.3, the damped natural frequencies were calculated to be: 2963 RPM ($p = -0.34$ rad/sec) for the forward mode and 3636 RPM ($p = -19.8$ rad/sec) for the backward whirl mode where p is the damping exponent of the corresponding critical speed. The mode shapes for the corresponding forward and backward modes of the first critical speed are given in Figs. 3 and 4. Note that the first critical speed backward mode shape given in Fig. 4 is quite similar to the conventional free–free undamped critical speed mode. But this mode will not be easily excited due to its high damping exponent values while the first forward mode with p almost zero is close to the stability threshold. This means that the rotor

is marginally stable and has a very high rotor amplification factor and hence may cause a large rotor unbalance response at the first critical speed. Using Eq. (2.8) and Eq. (2.10), the rotor first forward resonance speed and its corresponding amplification factor are computed to be

$$N_{ul}^{f}=\frac{310^2+0.36^2}{310^2-0.36^2}\times\frac{60}{2\pi}=2962\ \text{RPM}$$

$$A_{ul}^{f}=\frac{310^2+0.36^2}{2\times0.36\times310}=430\,.$$

Similarly, the rotor backward resonance speed and amplification factor are computed to be $N_{u_1}^{b}=3651$ RPM and $A_{u_1}^{b}=9.64$. Thus it can be seen that the forward mode has a much higher amplification factor than the backward mode and will be very easy to excite.

Similar modal calculations show that the second damped natural frequency will have a forward critical speed at 4950 RPM ($p=-106.2$ rad/sec) and backward critical speed at 13918 RPM ($p=-7.03$ rad/sec). In this case, the backward critical speed occurs at a much higher speed than the forward critical speed (even higher than the third forward damped critical speed of 6750 RPM).

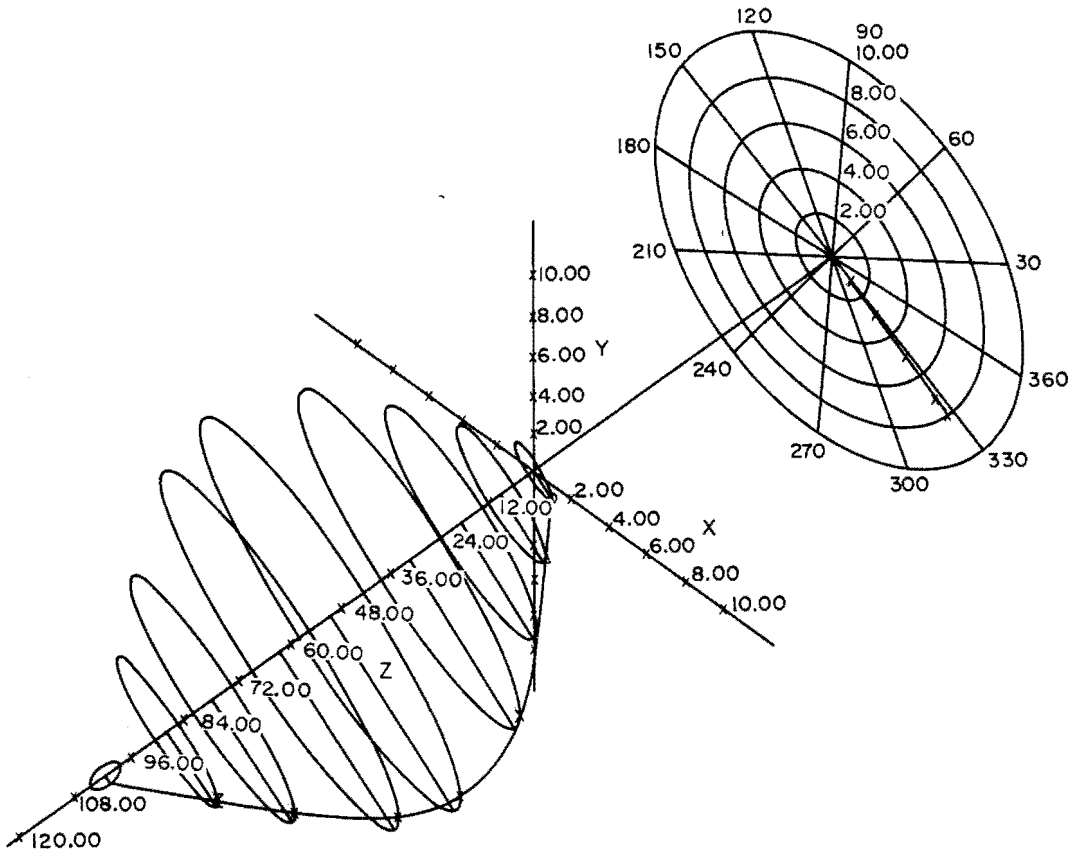

FIG. 3. First damped forward mode shape of the compressor.

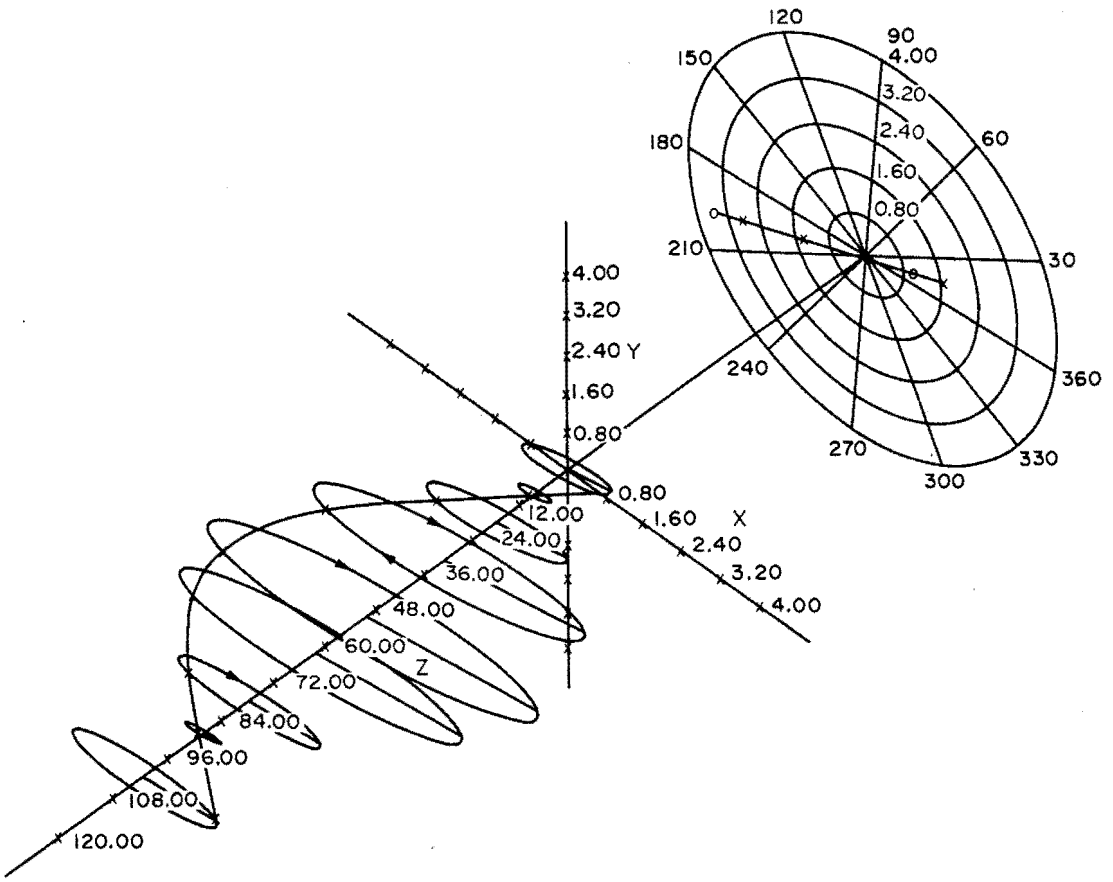

FIG. 4. First damped backward mode shape of the compressor.

The forward and backward mode shapes of the second damped critical speed are given in Figs. 5 and 6. Note that in Fig. 6 that the second backward mode shape is similar to conventional fourth bending mode because the second and third backward critical modes are critically damped over their critical speed range (**11**). The resonance speeds and amplification factor were calculated by Eq. (2.8) and Eq. (2.10) to be $N_{u2}^f = 5270$ RPM and $N_{u2}^b = 13198$ RPM and $A_{u2}^f = 2.54$ and $A_{u2}^b = 103.6$. Thus in the case of second mode resonance speed, the backward mode has a much higher speed than the forward mode and is much easier to be excited as discussed by Lund (**11**).

A computer program to calculate the damped natural frequencies using a matrix transfer method similar to that presented by Lund (**11**) was set up and the same industrial compressor analyzed. The first damped natural frequency was calculated to be 2960 RPM (forward) with $p = -0.36$ rad/sec and 3620 RPM (backward) with $p = -18.2$ rad/sec and are similar to the modal method calculations. A comparison of the first and second mode calculations by both modal and transfer matrix methods are given in Table II and they are in very good agreement.

The modal method was also applied to the unbalance response of the compressor. An unbalance of 1 oz-in. was placed in the mid-span between the bearings to simulate a first mode excitation using the modal approach discussed in Section II.4. The rotor unbalance response was calculated for an operating

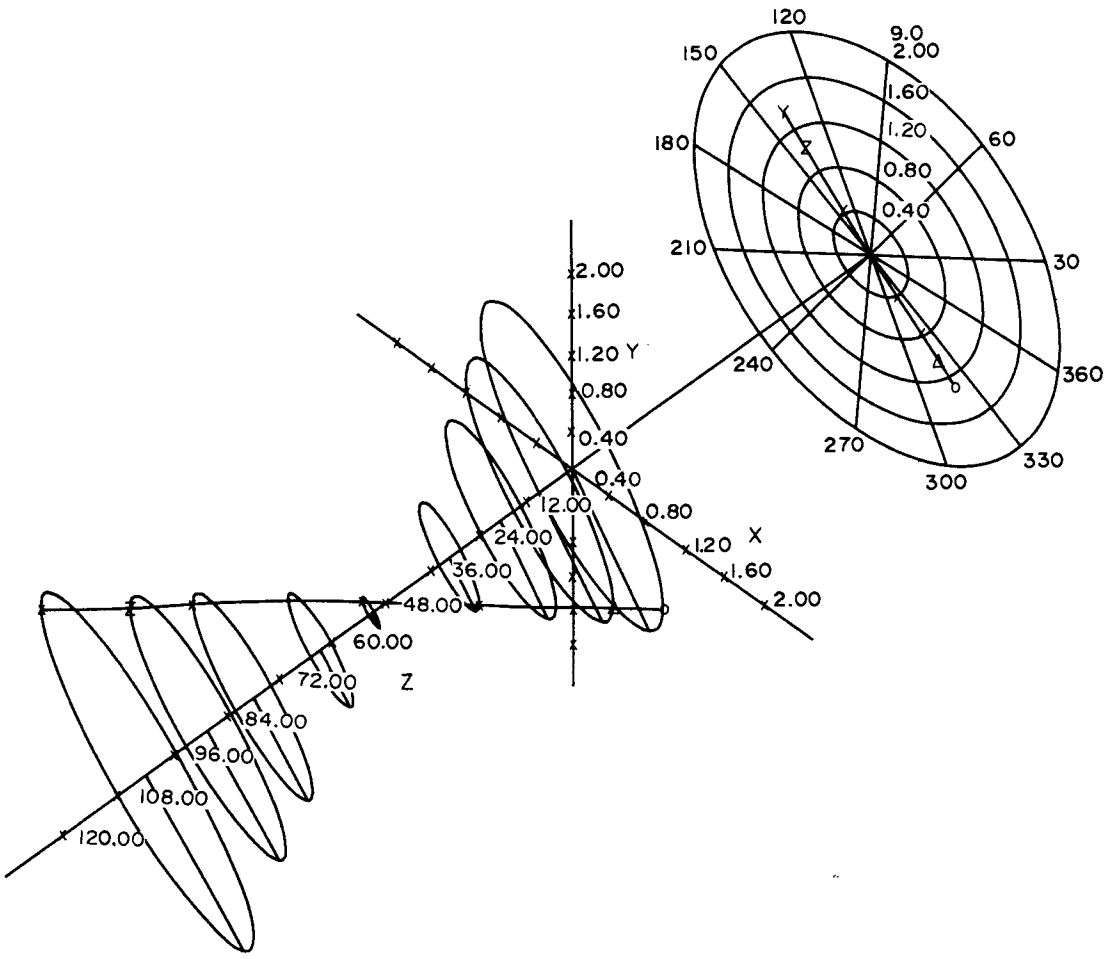

FIG. 5. Second damped forward mode shape of the compressor.

speed range of 500 RPM to 4500 RPM. For validation purposes, unbalance response calculations based on matrix transfer method were also performed. Figure 7 shows the comparisons of unbalance response calculated by both methods at the left bearing station and Fig. 8 shows the unbalance response at the mid rotor span. It can be seen from the figures that the results from both methods are in very good agreement. Note from Fig. 8 that the peak of the curve occurs at 2995 RPM with an amplitude of 29 mils. This peak response speed is very close to the calculation of $N_{u1} = 2963$ RPM using Eq. (2.8) while the undamped critical speed calculation indicates a critical speed of 3271 RPM. This does demonstrate that the undamped critical speed calculations may sometimes be quite misleading especially when moderate or large damping is incorporated into the system.

Another aspect of this analysis is that for a lightly damped system as this compressor, the unbalance response curve always gives a very sharp rising slope near the resonance speed or in other words, the speed range in which the peak resonance speed will occur is very narrow. For accurate calculations, the unbalance response of the system has to be calculated for very small speed increments so as to insure the peak response amplitude will not occur between two consecutive speed increments. Since each unbalance response calculation is

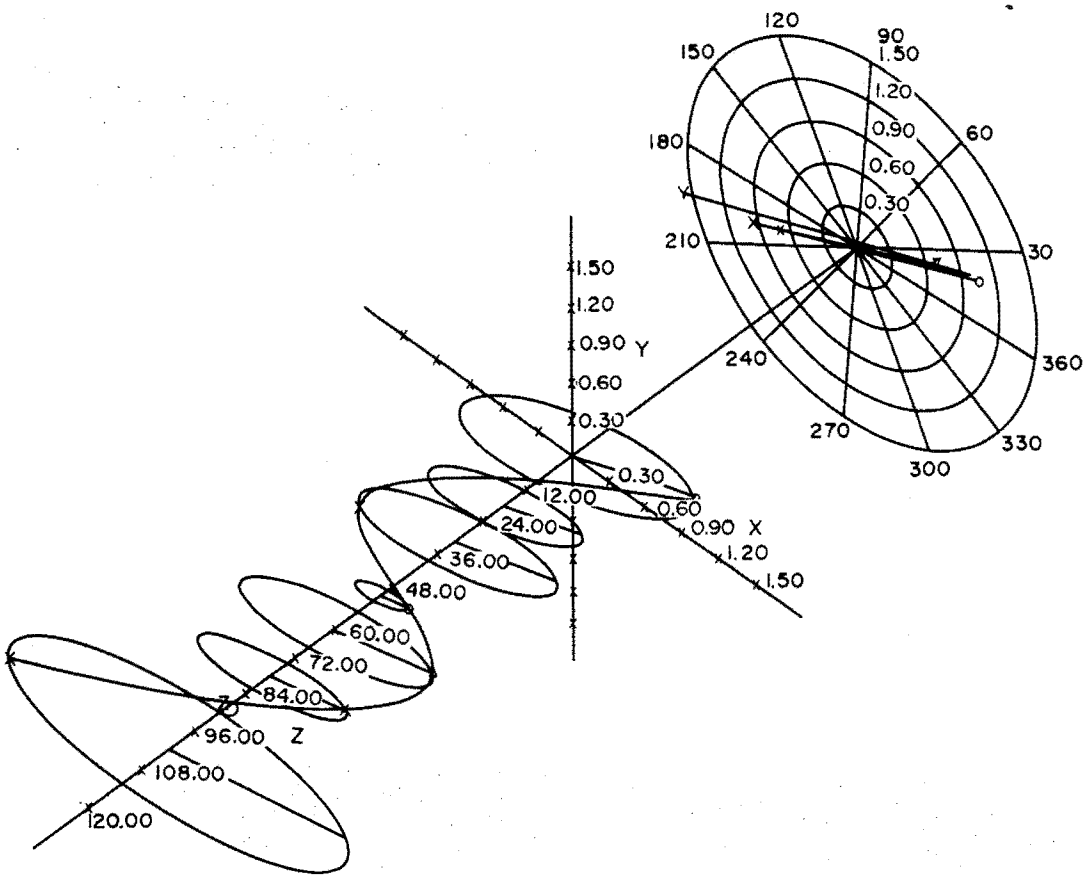

FIG. 6. Second damped backward mode shape of the compressor.

quite time consuming, this will make the analysis quite expensive. However, there is a fast method of approximating the maximum unbalance response amplitude using the amplification factors discussed previously. Using the concept that the peak response amplitude z_i is

$$z_i = e_i A_{ui} = 0.085 \times 430 = 36 \text{ mils}$$

where

$$\text{modal eccentricity } e_i = \frac{1 \text{ oz-in} \times 1000 \text{ mils/in}}{16 \text{ oz/lb} \times 740 \text{ lb}} = 0.085 \text{ mils}.$$

In this calculation, a modal weight of 740 lb for the first mode is used instead of the rotor total weight of 1400 lb.

The maximum amplitude of 36 mils calculated from rotor amplification factor is higher than the 29 mils calculation from unbalance response computer program. It appears that, in this case, even a speed increment of 1 RPM is still not small enough to catch the real peak of the resonance motion. The amplification factor can provide the designers information of the maximum rotor motion in a simplified manner.

TABLE II

			Mode 1	Mode 2
N_p (planar) average bearing stiffness			3270 RPM	7527 RPM
N_p (planar) horizontal bearing stiffness			3110 RPM	6541 RPM
N_p (planar) vertical bearing stiffness			3371 RPM	8419 RPM
Transfer matrix method	N_d	Forward	2690 RPM	4837 RPM
		Backward	3620 RPM	13900 RPM
	P	Forward	−0.36 rad/sec	−109 rad/sec
		Backward	−18.2 rad/sec	−8.86 rad/sec
Modal method	N_d	Forward	2936 RPM	4950 RPM
		Backward	3636 RPM	13918 RPM
	P	Forward	−0.34 rad/sec	−106.2 rad/sec
		Backward	−19.8 rad /sec	−7.03 rad/sec
	N_u	Forward	2962 RPM	5270 RPM
		Backward	3651 RPM	13918 RPM
	A_u	Forward	430	2.54
		Backward	9.64	103.6

IV. Conclusions

(1) The incorporation of moderate amount of bearing damping in the rotor system can cause a considerable shift of the rotor resonance speeds from the values predicted by the undamped critical speed calculation.

(2) Uncoupled modal analysis based on the assumption of proportional damping may simplify the modal equations of motion but it is often not accurate for rotor systems with seals or hydrodynamic bearings.

(3) Modal transformation of the generalized equations of motion into modal equations of motion using the undamped modes can significantly reduce the

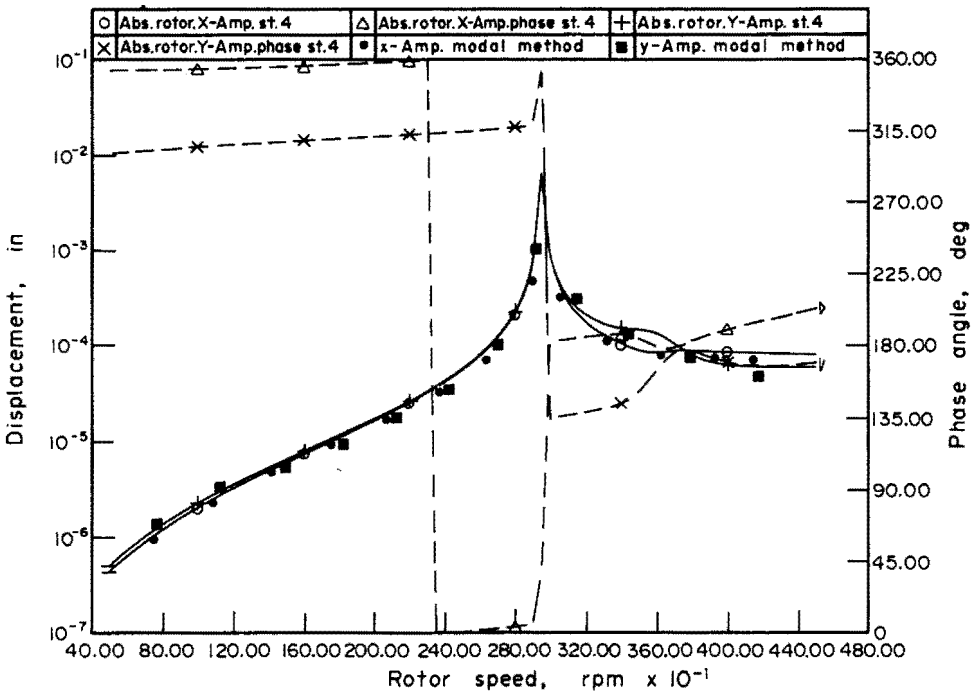

FIG. 7. Unbalance response plot of the compressor bearing station with first mode excitation.

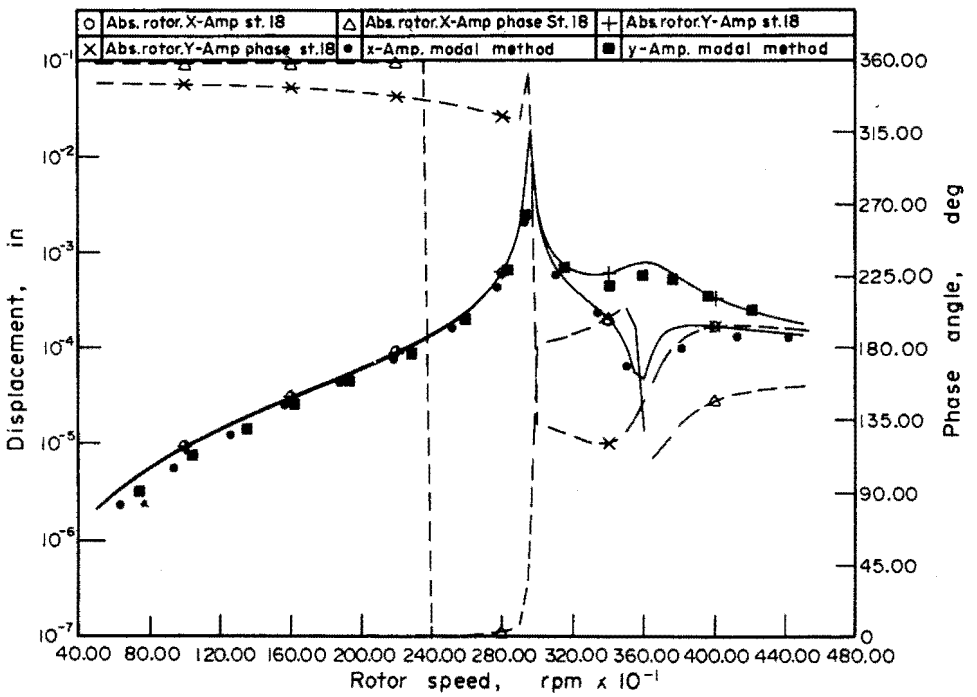

FIG. 8. Unbalance response plot of the mid-span of compressor rotor with first mode excitation.

TABLE III

Mode		Modal method	Matrix transfer method
	N_d RPM	6750	6692
3	P rad/sec	−144	−150
	A_u	2.55	
	N_d RPM	14033	14041
4	P rad/sec	−5.33	−5.93
	A_u	138	
	N_d RPM	27503	27571
5	P rad/sec	−86.8	−95.5
	A_u	16.6	

number of equations to be solved without losing the generalities of bearing cross-coupling effects and influence of gyroscopic moments.

(4) Damped complex eigenvalues, stability and unbalance response of the rotor system can be rapidly approximated using the undamped modes which are essential for design and are relatively easy to obtain by the designers.

(5) The combined effect of disc skew and rotor unbalance can be evaluated as a modal forcing function using both translational and rotational mode shapes. This modal forcing function can be used as a balancing parameter for complex multimass rotor with many discs.

(6) The use of one set of undamped modes calculated from the average bearing stiffness instead of using two sets of different modes in the x and y directions simplifies the modal calculations without losing much of its accuracy. It provides more physical insight of the rotor behavior than the use of the free-free mode shapes.

(7) Rotor bearing system resonance speeds and their corresponding amplification factors can be accurately approximated by simple calculations using the undamped modes.

(8) Extension of analysis to include effects of flexible casing can be achieved by present theory using the method of superposition of the undamped casing modes.

(9) The modal equations used for unbalance response calculations can also be used for modal transient analysis or simulation of turbine blade loss dynamics by applying appropriate initial conditions for numerical integration.

(10) Results indicate that the use of undamped planar mode shapes for industrial rotors may be more accurate than using free-free modes. This would enable the use of fewer modes.

Acknowledgements

The author would like to thank Mr. Lloyd Barrett for the development of the transfer matrix stability program, Mr. Alan Palazzolo for the development of the three dimensional plotting routine, and Mr. Dennis Li for the development of the transfer matrix unbalance response program. This work was supported in part by NASA Lewis Research Center Contract No. NSG-3104 under the direction of Dr. David Flemming and Energy Research and Development Agency Contract No. EF-76-5-01-2479.

References

(1) E. L. Thearle, "Dynamic Balancing of Rotating Machinery in the Field", *J. Appl. Mech.* APM-56-19, pp. 745–753, 1934.

(2) K. Foss, "Co-Ordinates Which Uncouple the Equations of Motion of Damped Linear Dynamic Systems", *J. Appl. Mech. Trans. ASME*, Sept. 1958.

(3) E. C. Pestel and F. A. Leckie, "Matrix Methods in Elastomechanics", McGraw-Hill, New York, 1963.

(4) J. W. Lund and F. K. Orcutt, "Calculations and Experiments on the Unbalance Response of a Flexible Rotor", *J. Engng. Industry, Trans. ASME*, Series B, Vol. 89, No. 4, pp. 785–796, Nov. 1967.

(5) R. E. D. Bishop and A. G. Parkinson, "Vibration and Balancing of Flexible Shafts", *Appl. Mechanics Reviews*, pp. 439–493, May 1968.

(6) K. Kikuchi, "Analysis of Unbalance Vibration of Rotating Shaft System with Many Bearings and Disks", *Bull. JSME*, Vol. 13, No. 61, pp. 864–872, June 1969.

(7) R. L. Ruhl and J. F. Booker, "A Finite Element Model for Distributed Parameter Turbototor Systems", *J. Engng. Industry, Trans. ASME*, Series B, Vol. 94, No. 1, pp. 126–132, Feb. 1972.

(8) W. Kellenberger, "Should a Flexible Rotor Be Balanced in N or $(N+2)$Planes?", *J. Engng. Industry, Trans. ASME*, pp. 548–560, May 1972.

(9) R. E. D. Bishop and A. G. Parkinson, "On the use of Balancing Machines for Flexible Rotors", *J. Engng. Industry*, May 1972.

(10) L. Barrett, P. Allaire and E. Gunter, "Unbalance Response of Flexible Rotors: Effect and Design of Flexible Damped Bearings", Report No. ME-543-106-74, May 1974, Dept. of Mechanical Engineering, University of Virginia, Charlottesville, Virginia.

(11) J. W. Lund, "Stability and Damped Critical Speeds of a Flexible Rotor in

Fluid-Film Bearings", *J. Engng. Industry, Trans. ASME*, pp. 509–517, May 1974.

(**12**) D. W. Childs, "A Rotor-Fixed Modal Simulation Model for Flexible Rotating Equipment", *J. Engng. Industry, Trans. ASME*, series B, Vol. 96, No. 2, pp. 659–669, May 1974.

(**13**) D. W. Childs, "Two Jeffcott-Based Modal Simulation Models for Flexible Rotating Equipment", *J. Engng. Industry*, ASME Paper No. 74-WA/DE-17, 1974.

(**14**) R. G. Kirk and E. J. Gunter, "Transient Response of Rotor–Bearing Systems", *J. Engng. Industry, Trans. ASME*, May 1974.

(**15**) P. N. Bansal and R. G. Kirk, "Stability and Damped Critical Speeds of Rotor Bearing Systems", *J. Engng. Industry*, Paper No. 75-DET-57.

(**16**) P. De Choudhury, S. J. Zsolcsak and E. W. Barth, "Effect of Damping on the Lateral Critical Speeds of Rotor Bearing Systems", *J. Engng. Industry, Trans, ASME*, Paper No. 75-DET-38, 1975.

(**17**) K. Choy and E. J. Gunter, "Unbalance Response and Modal Balancing of a Uniform Rotor", Report No. ME-543-125-75, Aug. 1975, Dept. of Mechanical Engineering, University of Virginia, Charlottesville, VA.

(**18**) J. W. Lund, "A Method for Using the Free Shaft Modes in Rotor Balancing", Conference on Vibrations in Rotating Machinery, Instn. Mech. Eng., pp. 65–72, Sept. 1976.

(**19**) H. F. Black and S. M. Nuttall, "Modal Resolution and Balancing of Sychronous Vibrations in Flexible Rotors with Non-Conservative Cross Coupling", Conference on Vibrations in Rotating Machinery, Instn. Mech. Engrs., pp. 151–158, Sept. 1976.

(**20**) A. G. Parkinson, "The Modal Interpretation of the Vibration of a Damped Rotating Shaft", Conference on Vibrations in Rotating Machinery, Instn. Mech. Engrs., pp. 263–278, Sept. 1976.

(**21**) W. C. Hurty and M. F. Rubinstein, "Dynamics of Structures", Prentice Hall, Englewood Cliffs, N. J., 1967.

(**22**) E. J. Gunter, "Dynamic Stability of Rotor-Bearing System", NASA Report SP-113, 1965.

(**23**) A. J. Dennis, R. H. Eriksson and L. H. Seitelman, "Transient Response Analysis of Damped Rotor System by the Normal Mode Method", ASME Paper No. 75-GT-58, 1975.

(**24**) M. Z. Prohl. "A General Method for Calculating Critical Speeds of Flexible Rotors", Trans. ASME, Vol. 67, *J. Appl. Mech.* Vol. 12, P. A–142, 1945.

Appendix A.

The equation of motion for the ith disc of a general multimass rotor system may be obtained by summing the inertia and external forces and moments acting at the ith station. The external forces and moments acting on the disc may in general be composed of elastic shaft reactions, unbalance forces, bearing or seal forces, or other external hydraulic forces acting on the system. A schematic of the forces and moments acting at the ith station is given in Fig. 9. The resulting basic equations of motion of the disc are (**14**):

Summation of forces in x-direction

$$m_i\ddot{X}_i + V^L_{ix} - V^R_{i-1x} + F_{bx}(X, Y, \theta, \psi, \dot{X}, \dot{Y}, \dot{\theta}, \dot{\psi}) = F_x(t). \tag{A.1}$$

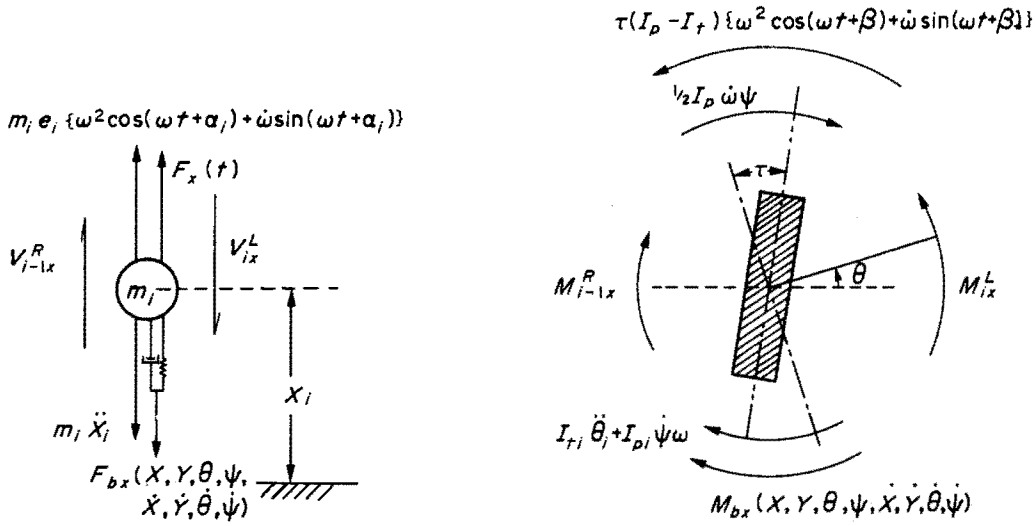

FIG. 9. Free-body diagram of forces and moments acting at mass station.

Summation of forces in y-direction

$$m_i \ddot{Y}_i + V^L_{iy} - V^R_{i-1y} + F_{by}(X, Y, \theta, \psi, \dot{X}, \dot{Y}, \dot{\theta}, \dot{\psi}) = F_y(t). \tag{A.2}$$

Summation of moments at the ith station

$$I_{ti}\ddot{\theta}_i + I_{pi}\dot{\psi}\omega + M^R_{i-1x} - M^L_{ix} + \tfrac{1}{2} I_p \dot{\omega}\psi + M_{bx}(X, Y, \theta, \psi, \dot{X}, \dot{Y}, \dot{\theta}, \dot{\psi}) = M_y(t) \tag{A.3}$$

$$I_{ti}\ddot{\psi}_i - I_{pi}\dot{\theta}\omega + M^R_{i-1y} - M^L_{iy} - \tfrac{1}{2} I_p \dot{\omega}\psi + M_{by}(X, Y, \theta, \psi, \dot{X}, \dot{Y}, \dot{\theta}, \dot{\psi}) = M_y(t). \tag{A.4}$$

For an unbalanced rotor with a skewed disc, the external time dependent forcing functions are of the form

$$\begin{Bmatrix} F_x(t) \\ F_y(t) \end{Bmatrix} = m_i e_i \left\{ \omega^2 \begin{bmatrix} \cos(\omega t+\alpha_i) \\ \sin(\omega t+\alpha_i) \end{bmatrix} + \dot{\omega} \begin{bmatrix} \sin(\omega t+\alpha_i) \\ -\cos(\omega t+\alpha_i) \end{bmatrix} \right\} \tag{A.5}$$

$$\begin{Bmatrix} M_x(t) \\ M_y(t) \end{Bmatrix} = \tau(I_p - I_t)_i \left\{ \omega^2 \begin{bmatrix} \cos(\omega t+\beta_i) \\ \sin(\omega t+\beta_i) \end{bmatrix} + \dot{\omega} \begin{bmatrix} \sin(\omega t+\beta_i) \\ -\cos(\omega t+\beta_i) \end{bmatrix} \right\} \tag{A.6}$$

where α_i and β_i represent the angle of the unbalance vector and disc skew with respect to the shaft reference mark.

The shear and moment relations are given by

$$V^L_{ix} = V^R_{ix} = \left(\frac{6EI}{L^3}\right)_i \left[2X_i + \theta_i L_i - 2X_{i+1} + \theta_{i+1} L_i\right] \tag{A.7}$$

$$M^L_{ix} = \left(\frac{2EI}{L^2}\right)[-3x_i - 2\theta_i L_i + 3x_{i+1} - \theta_{i+1} L_i] \tag{A.8}$$

$$M^R_{ix} = L_i V^{L'}_{ix} + M^L_{ix}. \tag{A.9}$$

The free boundary conditions at the ends of the shaft are

$$\{V^R_0 = M^R_0 = V^L_n = M^L_n\}_{x,y} = 0.$$

Let

$$\{U\} = \begin{Bmatrix} (X) \\ (\theta) \\ (Y) \\ (\psi) \end{Bmatrix}$$

and the general equation of motion for the rotor system can be expressed as

$$[\bar{M}]\{\ddot{U}\} + [C]\{\dot{U}\} + [K]\{U\} = \{F(t)\} \tag{A.10}$$

where

$$[\bar{M}] = \begin{bmatrix} [M] & o & 0 & 0 \\ 0 & [I_t] & 0 & 0 \\ 0 & 0 & [M] & 0 \\ 0 & 0 & 0 & [I_t] \end{bmatrix}.$$

For the case of linear bearings, the general damping matrix may be decomposed into the gyroscopic and the bearing damping submatrices as follows

$$[C] = \begin{bmatrix} 0 & 0 & 0 & 0 \\ 0 & 0 & 0 & 0 \\ 0 & 0 & 0 & [\frac{1}{2}Ip\omega] \\ 0 & [-\frac{1}{2}Ip\omega] & 0 & 0 \end{bmatrix} + \begin{bmatrix} [C_{xx}] & [C_{x\theta}] & [C_{xy}] & [C_{x\psi}] \\ [C_{\theta x}] & [C_{\theta\theta}] & [C_{\theta y}] & [C_{\theta\psi}] \\ [C_{yx}] & [C_{y\theta}] & [C_{yy}] & [C_{y\psi}] \\ [C_{\psi x}] & [C_{\psi\theta}] & [C_{\psi y}] & [C_{\psi\psi}] \end{bmatrix}.$$

The general stiffness matrix may also be decomposed into three sub-matrices representing the symmetric shaft stiffness matrix, the linear bearing stiffness matrix and the skew symmetric acceleration matrix as follows

$$[K] = \begin{bmatrix} [k_{xx}] & [k_{x\theta}] & 0 & 0 \\ [k_{x\theta}] & [k_{\theta\theta}] & 0 & 0 \\ 0 & 0 & [k_{xx}] & [k_{x\theta}] \\ 0 & 0 & [k_{x\theta}] & [k_{\theta\theta}] \end{bmatrix}_s + \begin{bmatrix} [K_{xx}] & [K_{x\theta}] & [K_{xy}] & [K_{x\psi}] \\ [K_{\theta x}] & [K_{\theta\theta}] & [K_{\theta y}] & [K_{\theta\psi}] \\ [K_{yx}] & [K_{y\theta}] & [K_{yy}] & [K_{y\psi}] \\ [K_{\psi x}] & [K_{\psi\theta}] & [K_{\psi y}] & [K_{\psi\psi}] \end{bmatrix}_b$$

$$+ \begin{bmatrix} 0 & 0 & 0 & 0 \\ 0 & 0 & 0 & [\frac{1}{2}Ip\dot{\omega}] \\ 0 & 0 & 0 & 0 \\ 0 & [-\frac{1}{2}Ip\dot{\omega}] & 0 & 0 \end{bmatrix}$$

where

$$[k_{xx}] = 2\begin{bmatrix} E_1 & -E_2 & 0 & \dots & 0 & 0 \\ -E_1 & E_1+E_2 & -E_2 & \dots & 0 & 0 \\ \dots & \dots & \dots & \dots & \dots & \dots \\ 0 & 0 & 0 & \dots & -E_{n-1} & E_{n-1} \end{bmatrix}$$

for

$$E_i = \left(\frac{6EI}{L^3}\right)_i$$

$$[k_{x\theta}]=[k_{\theta x}]^T=\begin{bmatrix} E_1L_1 & E_1L_1 & 0 & \dots & 0 & 0 \\ -E_1L_1 & -E_1L_1+E_2L_2 & E_2L_2 & \dots & 0 & 0 \\ & & & & & \\ 0 & 0 & & \dots & -E_{n-1}L_{n-1} & -E_{n-1}L_{n-1} \end{bmatrix}$$

and

$$[k_{\theta\theta}]=\frac{1}{3}\begin{bmatrix} 2E_1L_1^2 & E_1L_1^2 & 0 & \dots & 0 & 0 \\ E_1L_1^2 & 2E_1L_1^2+2E_2L_2^2 & E_2L_2^2 & \dots & 0 & 0 \\ & & & \dots & & \\ 0 & 0 & \dots & \dots & E_{n-1}L_{n-1}^2 & 2E_{n-1}^2L_{n-1} \end{bmatrix}.$$

Note that for a circular shaft, the symmetric shaft stiffness matrix is identical for both x and y directions. If the rotor gyroscopic effects, bearing damping and stiffness cross-coupling effects are ignored, the above dynamic equations can be rewritten as follows:

$$\begin{bmatrix}[M] & 0 \\ 0 & [I_t]\end{bmatrix}\begin{Bmatrix}\ddot{X} \\ \ddot{\theta}\end{Bmatrix}+\begin{bmatrix}[K_b] & 0 \\ 0 & 0\end{bmatrix}\begin{Bmatrix}X \\ \theta\end{Bmatrix}+\begin{bmatrix}[k_{xx}] & [k_{x\theta}] \\ [k_{\theta x}] & [k_{\theta\theta}]\end{bmatrix}\begin{Bmatrix}X \\ \theta\end{Bmatrix}=\begin{Bmatrix}0 \\ 0\end{Bmatrix} \tag{A.11}$$

where

$$[K_b]=\frac{[K_{xx}]_B+[K_{yy}]_B}{2}.$$

The solution to the above undamped homogeneous system leads to a set of orthogonal mode shapes Φ_i and their corresponding natural frequencies ω_i.

For modal analysis, let

$$\begin{bmatrix}\{X\} \\ \{\theta\} \\ \{Y\} \\ \{\psi\}\end{bmatrix}=\sum_{i=1}^{n}\begin{Bmatrix}q_{xi} & \{\Phi_i\} \\ q_{yi} & \{\Phi_i\}\end{Bmatrix}=\sum_{i=1}^{n}\begin{Bmatrix}q_{xi} \\ q_{yi}\end{Bmatrix}\begin{Bmatrix}\{\phi\} \\ \{\phi'\} \\ \{\phi\} \\ \{\phi'\}\end{Bmatrix}. \tag{A.12}$$

Premultiply equation (A.10) by $\{\Phi_i\}^T$ and apply orthogonality conditions of the mode shapes, the equations of motion can be written into a set of compact equations using summation convention as

$$\ddot{q}_{xi}+\omega_i^2q_{xi}+C_{ij}^x\dot{q}_{xj}+B_{ij}^xq_{xj}+D_{ij}^x\dot{q}_{yj}+E_{ij}^xq_{yj}=P_{xi} \tag{A.13}$$

and there is a similar set of equations for the y–z plane as follows:

$$\ddot{q}_{yi}+\omega_i^2q_{yi}+C_{ij}^y\dot{q}_{yj}+B_{ij}^yq_{yj}+D_{ij}^y\dot{q}_{xj}+E_{ij}^yq_{xj}=P_{yi} \tag{A.14}$$

where

$$P_{xi}=\phi_i^TMe[\omega^2\cos(\omega t+\alpha)+\dot{\omega}\sin(\omega t+\alpha)]$$
$$+\phi_i'^T\tau(I_p-I_t)[\omega^2\cos(\omega t+\beta)+\dot{\omega}\sin(\omega t+\beta)] \tag{A.15}$$

B_{ij}, C_{ij}, D_{ij}, E_{ij} are modal cross-coupling terms from disc gyroscopic, bearing cross-

coupling stiffness, and damping effects. For example, the modal damping coefficient C_{ij}^{x} can be calculated as

$$C_{ij}^{x} = \{\phi_i\}^T[C_{xx}]\{\phi_j\} + \{\phi_i\}^T[C_{x\theta}]\{\phi_j'\} + \{\phi_i'\}^T[C_{\theta x}]\{\phi_j\} + \{\phi_i\}^T[C_{\theta\theta}]\{\phi_j\}. \quad \text{(A.16)}$$